Nuclear Science and Techniques (2024) 35:109
https://doi.org/10.1007/s41365-024-01473-7

Carbon-based nanomaterials cause toxicity by oxidative stress to the liver and brain in Sprague–Dawley rats

Ying-Ying Xu[1] · Chan Jin[2] · Meng Wu[2] · Jian-Ye Zhou[3] · Hui-Ling Wei[3]

Received: 18 September 2023 / Revised: 9 December 2023 / Accepted: 2 January 2024 / Published online: 4 July 2024

Abstract

Carbon-based nanomaterials have important research significance in various disciplines, such as composite materials, nanoelectronic devices, biosensors, biological imaging, and drug delivery. Recently, the human and ecological risks associated with carbon-based nanomaterials have received increasing attention. However, the biological safety of carbon based nanomaterials has not been systematically studied. In this study, we used different types of carbon materials, namely, graphene oxide (GO), single-walled carbon nanotubes (SWCNTs), and multiwalled carbon nanotubes (MWCNTs), as models to observe their distribution and oxidative damage in vivo. The results of Histopathological and ultrastructural examinations indicated that the liver and lungs were the main accumulation targets of these nanomaterials. SR-μ-XRF analysis revealed that SWCNTs and MWCNTs might be present in the brain. This shows that the three types of carbon-based nanomaterials could cross the gas–blood barrier and eventually reach the liver tissue. In addition, SWCNTs and MWCNTs could cross the blood–brain barrier and accumulate in the cerebral cortex. The increase in ROS and MDA levels and the decrease in GSH, SOD, and CAT levels indicated that the three types of nanomaterials might cause oxidative stress in the liver. This suggests that direct instillation of these carbon-based nanomaterials into rats could induce ROS generation. In addition, iron (Fe) contaminants in these nanomaterials were a definite source of free radicals. However, these nanomaterials did not cause obvious damage to the rat brain tissue. The deposition of selenoprotein in the rat brain was found to be related to oxidative stress and Fe deficiency. This information may support the development of secure and reasonable applications of the studied carbon-based nanomaterials.

Keywords Carbon-based nanomaterials · Oxidative stress · Trace element distribution · TEM · SR-μ-XRF

1 Introduction

Nanotechnology has revolutionized everything from production to health. Currently, carbon-based nanomaterials have emerged as a global research hotspot [1–3]. Ideal carbon nanotubes (CNTs) are a new type of nanomaterial that usually use a multilayer composite structure from a single layer to more than 100 layers. CNTs with one graphene layer and those with more than one layer are called single-walled carbon nanotubes (SWCNTs) and multiwalled carbon nanotubes (MWCNTs), respectively. Owing to their excellent aspect ratios and electrical, mechanical, and physicochemical properties, they have been applied in various research fields, such as composite materials [4, 5], nanoelectronic devices [6], biological sensors [7], biological imaging [8, 9], and biomedicine [10, 11]. In addition, carbon-based nanomaterials can be used as a new type of transport for a variety of peptides, proteins, plasmid DNAs, and SiRNA in the biomedical field [12, 13]. CNTs have demonstrated good modifiability, which has good application prospects in diagnosis, invisibility, targeting, and drug loading. Interestingly, it is worth mentioning that in 2013, the worldwide production of MWCNTs and SWCNTs was approximately 2000 tons and 6 tons, respectively [14], which would be is expected

This work was supported by the National Natural Science Foundation of the Henan University (21IRTSTHN011).

✉ Ying-Ying Xu
15901033816@163.com

[1] Department of Gastroenterology, China-Japan Friendship Hospital, Beijing 100029, China

[2] Shanghai Institute of Applied Physics, Chinese Academy of Sciences, Shanghai 201800, China

[3] Institute of Particle and Nuclear Physics, College of Physics, Henan Normal University, Xinxiang 453007, China

to exceed 20,000 tons (SWCNTs and MWCNTs combined) in 2022. The increasing popularity and production of CNTs will inevitably lead to contact between the environment and human body. Thus, the toxicity of carbon-based nanoparticles is a notable challenge requiring further investigation.

Although the toxicological mechanism of carbon-based nanomaterials remains unclear, oxidative stress is considered to be one of the main causes of their toxicological effects [15–17]. It is characterized by excess reactive oxygen species (ROS) caused by a redox state imbalance [18]. Previous studies have demonstrated that carbon-based nanomaterials cause significant damage to the liver, kidneys, and brain, which are sensitive to oxidative stress [19–22]. In addition, the instillation of carbon-based nanoparticles in rats could result in lung injury, accompanied by obvious inflammatory and fibrotic features, which might be due to the accumulation of black foreign substances in the lungs. Wang et al. [23] demonstrated that SWCNTs accumulated in small doses in vascular endothelial cells and in the bone, stomach, and kidney for a long time in animals. Furthermore, it had been reported that MWCNTs could cross most of the biological barriers after tail vein administration, including the blood–brain barrier (BBB) [24, 25]. However, owing to the various exposure routes, there is no significant difference in the distribution of carbon-based nanomaterials in the body [23], which is closely related to their transport capacity in the body [26]. In addition, several neurotoxicological mechanisms have been associated with cell homeostasis and trace elements [27–30], as well as free radical production [31]. The interaction between nanomaterials and trace elements, particularly selenium (Se), which is known as an antioxidant, has an antagonistic effect on nanomaterials [32]. Synchrotron micro-X-ray fluorescence (μ-XRF) with a high spatial resolution is an excellent technique for elemental spatial distribution [33, 34]. However, the mechanism underlying spatial distribution and cross-cellular transport of carbon-based nanomaterials in vivo remains unclear, especially regarding the cytotoxicity caused by the oxidative stress of carbon-based nanoparticles in vivo.

In light of the above, in this study, Sprague–Dawley (SD) rats intratracheally instilled with different concentrations of graphene oxide (GO), SWCNTs, and MWCNTs were used as models to confirm the toxicity of carbon-based nanomaterials including oxidative stress and its distribution. Its location in the tumor tissue was determined by histopathological, ultrastructural, and SR-μ-XRF examinations. We then focused on the oxidative stress and antioxidant status in the liver and brain. Furthermore, the major trace element spatial distribution of calcium (Ca), iron (Fe), and Se in the rat brain was evaluated. These data support the development of secure and reasonable applications.

2 Materials and methods

2.1 The properties of carbon-based nanomaterials

GO was prepared using the improved Hummer method [35, 36], and SWCNTs and MWCNTs were synthesized using catalytic chemical vapor deposition technology [37]. All the carbon-based nanomaterials were obtained from the Institute of Chemistry, Chinese Academy of Sciences. The characterization results are summarized in Table 1. After UV irradiation for 2 h, the carbon-based nanomaterials were suspended in normal saline to obtain concentrations of 50, 100, and 200 μg/mL. The suspension was ultrasonicated for 20 min, with a break every 10 min before use. The morphology and structure of the samples were observed using transmission electron microscopy (TEM, Hitachi-7650).

2.2 Animals and treatment

Sixty normal male SD rats were purchased from the Experimental Animal Research Center of the Chinese Academy of Sciences (Shanghai, China) and fed in two animal cages under a 12 h light/dark cycle. The cultural environment was as follows: the temperature was 23 °C to 26 °C, and the relative humidity was 50% to 60%. A supply of pure water and sterilized food was available.

The SD rats were randomly divided into 10 groups ($n = 6$).

(1) Normal group (GI): The members of this group received normal saline.
(2) GO-treated group (GII): Members of this group received GO (50, 100, and 200 μg/mL).
(3) SWCNT-treated group (GIII): The members of this group received SWCNTs (50, 100, and 200 μg/mL).
(4) MWCNT-treated group (GIV): The members of this group received MWCNTs (50, 100, and 200 μg/mL).

A suspension of 1.0 mL was instilled into the trachea of the rats using chloraldehyde hydrate as the anesthetic. The rats returned to their normal health within 30 days and were then euthanized. The lungs, liver, and brain were immediately collected and protected according to the determination

Table 1 The characterization of carbon-based nanomaterials

	SWCNTs	MWCNTs	GO
Diameter (nm)	2	10–20	< 500
Purity	> 90 wt.% carbon	> 95 wt.% carbon	–
	< 10 wt.% Fe	< 5 wt.% Fe	–
Length (μm)	5–15	5–15	–

requirements. All operations were performed in accordance with the standards of the China-Japan Friendship Hospital and strictly in accordance with the principle of relieving pain in rats.

2.3 Pathological and EM examination

The lung and liver tissues of the rats were removed, washed with an aqueous phosphoric acid solution, and fixed with 10% neutral buffered formalin (Shanghai Guoyao Chemical Company, China) for 2 days. The phosphate-buffered saline (PBS) washing method was used to dry in the presence of a certain amount of alcohol and wrapped in paraffin, and 5 microns were stained with hematoxylin–eosin (H &E). Finally, pathological changes in the lungs and liver were observed under a microscope (Leica Microsystems, Germany).

2.4 Transmission electron microscopy (TEM)

The liver blocks were fixed with 2.5% glutaraldehyde (Shanghai National Pharmaceutical and Chemical Company) for 4 h, washed with PBS thrice, and treated with 1% cerium oxide for 1 h. Then, according to standard practice, the liver samples were washed with PBS, dried in a certain proportion, and embedded in epoxy resin. An ultramictotome (UC6, Leica), used to cut the samples, was mounted on copper grids, stained with uranyl acetate and lead citrate, and observed using TEM (TEM, Hitachi-7650).

2.5 Evaluation of oxidative stress and antioxidant status in rat liver and brain tissues

Rat liver and brain tissues were homogenized in 50 mM Tris-10 mM EDTA buffer (pH 7.4) and centrifuged at 13000×g at 4 °C for 30 min. Indices of oxidative stress and antioxidant status, namely, superoxide dismutase (SOD), catalase (CAT), malondialdehyde (MDA), glutathione (GSH), lactate dehydrogenase (LDH), and ROS, were measured. The activities of SOD and CAT were measured using SOD (Nanjing Jiancheng Bioengineering Institute) and CAT assay kits (Beyotime Institute of Biotechnology), respectively. The products of lipid peroxidation was analyzed using an MDA assay kit (Nanjing Jiancheng Bioengineering Institute). GSH levels were measured using the manufacturer's protocols specified in the GSH assay kit (Nanjing Jiancheng Bioengineering Institute). LDH leakage, used to measure membrane damage, was determined using a commercial LDH kit (Beyotime Institute of Biotechnology, Jiangsu). Finally, ROS levels were determined using ROS reagent kits (Beyotime Institute of Biotechnology, China). All the testing procedures were performed according to the manufacturer's instructions. A minimum of three trials were conducted each time.

2.6 Synchrotron radiation-induced micro X-ray fluorescence analysis (SR μ-XRF) analyses

The distributions of Ca, Fe, and Se in the brain sections were studied using μ-XRF at BL15U1 at the Shanghai Synchrotron Radiation Facility (SSRF) [27, 38]. In the storage ring, the energy of the electron beam was approximately 3.5 GeV, and the beam current was approximately 200 mA. During the experiment, the sample slice was placed on a sample holder in which the stepper motor driven by the microcomputer moved in both X- and Y-directions. The distributions of Ca, Fe, and Se in the brain slices were continuously observed at steps of 30 μm in both *X*- and *Y*-directions. Ten parallel scans on the brain samples were detected at a resolution of 30 μm × 30 μm from the edge to center, with an area of approximately 5.5 mm × 8.0 mm. The emission energy was 16.5 keV, and the collection speed was 1.0 s/step. Elemental fluorescence intensities were normalized to the ionization chamber signals, which were collected simultaneously. The X-ray spectra were analyzed using IGORPRO6.10 (Waveguide Materials Co., Ltd.).

2.7 Statistical analysis

All data were calculated as the mean ±standard deviation. One-way ANOVA and Dunnett's test were used to compare the groups. A significant difference was detected between the two groups ($P > 0.05$).

3 Results

3.1 Carbon-based nanomaterial characterization

The morphology and structure of the carbon-based nanocrystals were determined using TEM, as shown in Fig. 1. The GO particle size was approximately 400 nm, and clusters were easily formed. As shown in Fig. 1b and c, the SWCNT and MWCNT samples were easily entangled and difficult to separate using ultrasonic vibration. This result is consistent with previous reports [39, 40].

3.2 Pulmonary inflammatory cell infiltration

The alveolar volume was normal, and there was no obvious pulmonary artery dilatation after normal saline treatment (Fig. 2a). Compared with the normal group (GI), more black foreign bodies appeared in the lungs of rats treated with carbon-based nanomaterials (GII, GIII, and GIV), as shown in Fig. 2b–d. Meanwhile, a large amount

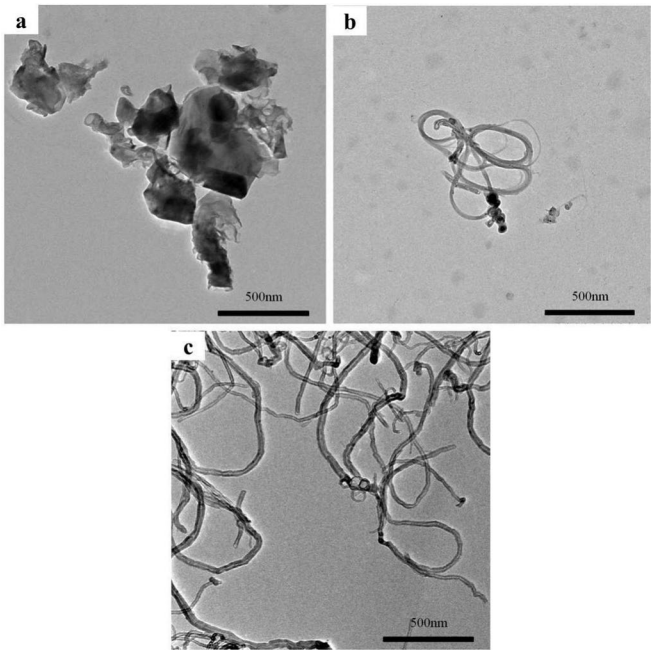

Fig. 1 Microphotograph of carbon-based nanomaterials. **a** GO; **b** SWCNTs; **c** MWCNTs

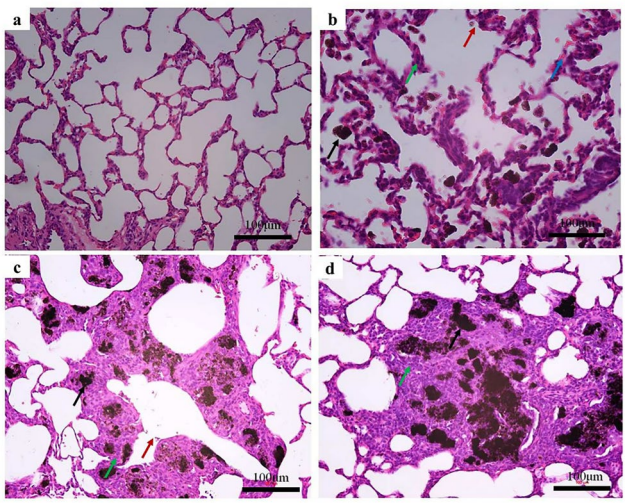

Fig. 2 (Color online) The histopathological changes in rat lung (HE staining, magnification × 100, Scale bar = 100 μm). **a** GI group; **b** GII group (100 μg/mL); **c** GIII group (100 μg/mL); **d**: GIV group (100 μg/mL); The green, red, blue and black arrows indicate inflammatory cell infiltration, epithelial cell necrosis, hyperemia, and carbon-based materials, respectively

of inflammatory cell infiltration was observed in the lung tissue. A few black foreign bodies are observed in the alveolar ducts of the GII group, as shown in Fig. 2b. They are characterized by irregular sizes and sunken alveoli. However, significant black foreign bodies were still observed in the bronchi of patients in the GIII and GIV groups, as shown in Fig. 2c and d. In the alveolar cavity, there were neutrophils and some thickening in the alveolar cavity. These results show that carbon-based nanomaterials can induce inflammatory lung injury.

3.3 Hepatic inflammatory cell infiltration

The histopathological images showed an abnormal structure in the liver tissues of rats after exposure to carbon-based nanomaterials as shown in Fig. 3a–d. Compared with the GI group, irregular arrangements of liver tissue, changes in vacuoles in the cytoplasm, and congestion and exudation of the portal vein in the liver tissue were observed after SWCNT and MWCNT exposure. Exudation of inflammatory cells was observed in the lesion, accompanied by local calcification. However, no significant changes were observed in the GII group. In addition, the liver tissue was observed using TEM as shown in Fig. 4a–d. After carbon-based nanomaterial exposure, we observed pathological changes such as nuclear pyknosis, mitochondrial swelling, and the loss of mitochondrial spines in the liver tissue of rats. Further studies revealed large numbers of small black substances in the mitochondrial cavity of rats in the GII group, while a large number of clusters of SWCNTs appeared in the mitochondrial cavity of the GIII group, which also showed that there was considerable blackness in the rat mitochondria in the GIV group. The results indicated that in blood circulation, carbon-based nanoparticles with different morphologies could be transported from the lungs to the liver tissue.

Although the liver histopathological examination revealed inflammatory damage and the presence of carbon-based materials, more oxidative stress is needed to confirm this conclusion. The oxidative stress levels in the livers of

rats treated with carbon-based nanomaterials are shown in Fig. 5a–f. ROS acted as a key factor for the stability of the biological environment. However, this process is highly fragile owing to the external stress. The results showed that

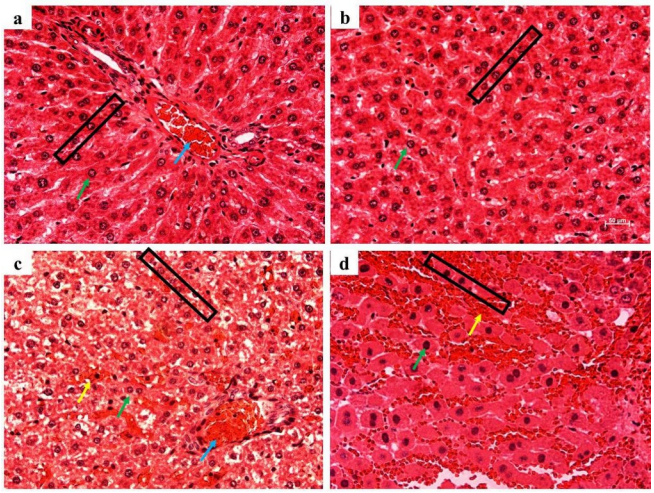

Fig. 3 (Color online) The histopathological changes in liver tissues of rats (HE staining, magnification × 200, Scale bar = 50 μm). **a** GI group; **b** GII group (100 μg/mL); **c** GIII group (100 μg/mL); **d** GIV group (100 μg/mL); The green, yellow, and blue arrows indicate hepatocytes, sinusoid capillary, and centrilobular veinule. The black boxes illustrate many hepatocytes arranged in the form of blades

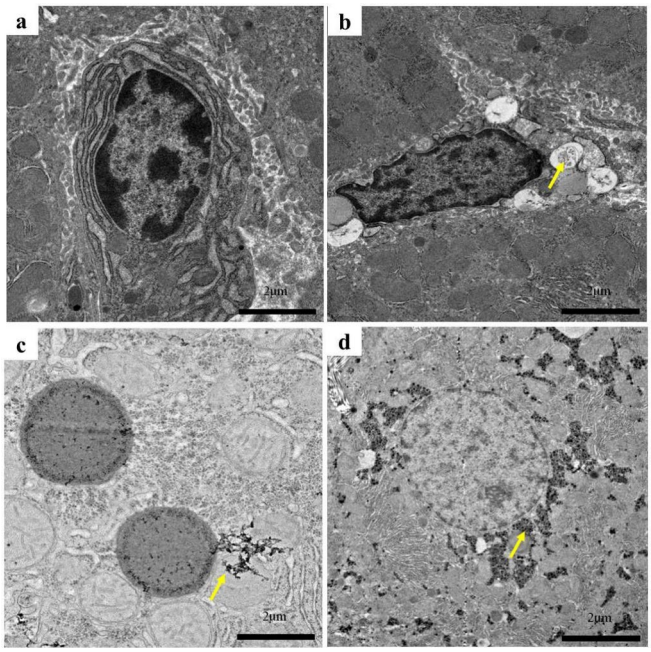

Fig. 4 (Color online) The ultrastructure changes in liver tissues of rats. **a** GI group; **b** GII group (100 μg/mL); **c** GIII group (100 μg/mL); **d** GIV group (100 μg/mL); The yellow arrows indicate black materials

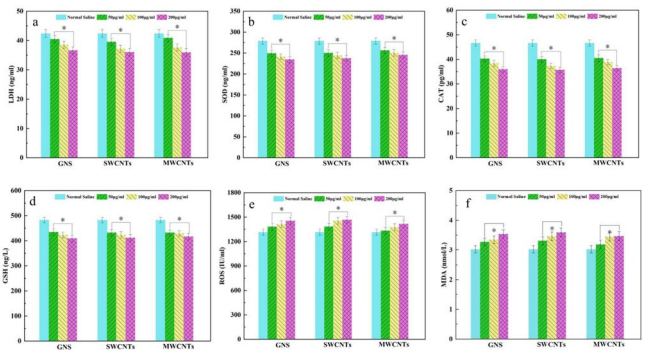

Fig. 5 (Color online) Effects of carbon-based nanomaterials on LDH, SOD, MDA, GSH, ROS, and CAT in rat livers. Values are means ±SD from at least three independent experiments ($n = 5$). $^{*}p < 0.03$, compared with the control group

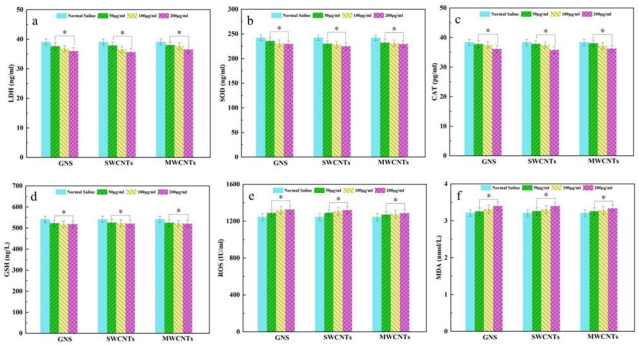

Fig. 6 (Color online) Effects of carbon-based nanomaterials on LDH, SOD, MDA, GSH, ROS, and CAT in rat brain. Values are means ±SD from at least three independent experiments ($n = 5$). $^{*}p < 0.03$, compared with the normal group

ROS levels increased significantly after treatment with carbon-based nanomaterials and were related to the increase in their concentration. Compared with the GI group, MDA levels were increased in the GII, GIII, and GIV groups, and MDA was assessed to be a lipid substance that could affect oxidative stress. In addition, the SOD and CAT, as the activity of antioxidant enzyme, decreased after carbon-based nanomaterial exposure. The results also showed that the degree of exposure and oxidation of the carbon-based nanomaterials were concentration-dependent. Compared with the GI group, the GSH level after carbon-based nanomaterials exposure displayed a reduction tendency, which exhibited the same trend as SOD and CAT. Furthermore, the results showed decreased generation of LDH in the GII, GIII, and GIV groups compared with that in the GI group. These studies showed that carbon-based nanomaterials can cause inflammatory damage and oxidative stress in rat liver tissues. In our carbon-based nanomaterial samples, a large number of Fe ions entered the samples during the synthesis process and were difficult to remove completely.

3.4 Neural inflammatory cell infiltration

To gain a deeper understanding of whether carbon-based nanomaterials caused damage to brain tissue through the blood system, the oxidative stress response and the spatial distribution of trace elements in the rat brain were determined using various methods. After exposure to carbon-based nanomaterials, the oxidative pressure response in the rat brain was measured, as shown in Fig. 6a–f. The results showed that MDA and ROS levels were slightly increased, and LDH, SOD, GSH, and CAT levels were decreased. In

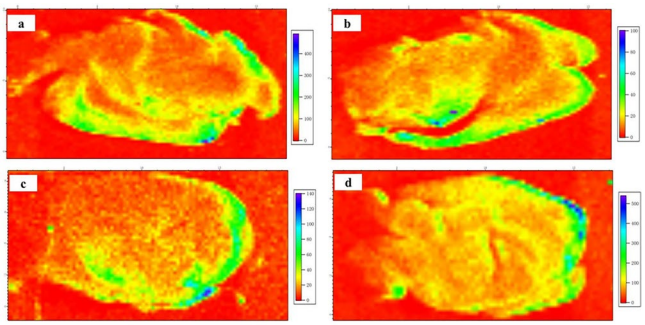

Fig. 7 (Color online) The SR-XRF images of Ca distribution in the brain section. **a** GI group; **b** GII group (100 μg/mL); **c** GIII group (100 μg/mL); **d** G IV group (100 μg/mL)

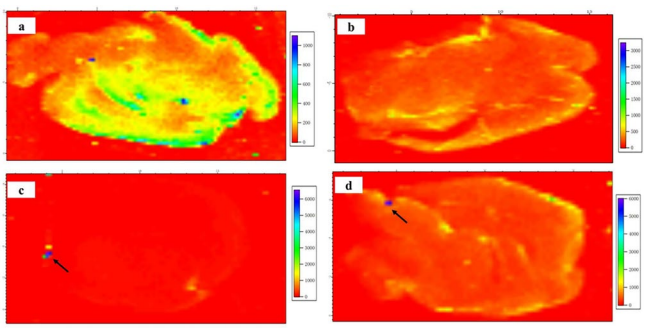

Fig. 8 (Color online) The SR-XRF images of Fe distribution in the brain section. **a** GI group; **b** GII group (100 μg/mL); **c** GIII group (100 μg/mL); **d** GIV group (100 μg/mL)

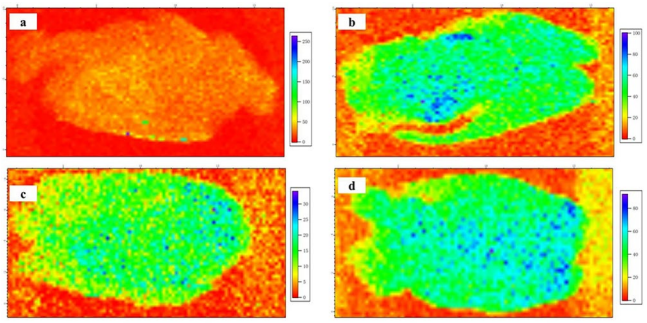

Fig. 9 (Color online) The SR-XRF images of Se distribution in the brain section. **a** GI group; **b** GII group (100 μg/mL); **c** GIII group (100 μg/mL); **d** GIV group (100 μg/mL)

this study, we found that different concentrations of carbon-based nanomaterials exerted some effect on oxidative damage to a certain extent; however, the degree of the effect was lower than that in normal rats.

The spatial distributions of Ca, Fe, and Se trace elements in the rat brain after carbon-based nanomaterial treatment were detected using SR μ-XRF as shown in Fig. 7, 8 and 9. The shapes and structures of these elemental images correspond very well with those of the brain sections. The spatial distribution of Ca in the brain sections of all three groups was similar, as shown in Fig. 7a–d, which was mostly rich in the cortex and slightly rich in other brain regions. No calcification was observed in the rat brain after carbon-based nanomaterial exposure. The Fe element was most rich in the cortex of brain sections in the control group, as shown in Fig. 8a. However, the Fe content decreased significantly in the brain sections after carbon-based nanomaterial treatment, as shown in Fig. 8b–d. Spots with high concentrations of Fe were observed in the groups exposed to SWCNTs and MWCNTs (Fig. 8c and d). The samples of SWCNTs and MWCNTs contained < 10wt.% Fe catalyst and < 5wt.% Fe catalyst, respectively. Therefore, the high concentration of Fe spots in the cortex may be due to SWCNTs and MWCNTs. Interestingly, the Se content increased significantly in the brain sections compared with the GI group, as shown in Fig. 9. Meanwhile, a larger amount of granular Se precipitation was observed in the brain sections after carbon-based nanomaterial treatment (Fig. 9b–d). In our results, oxidative stress in the rat brain after the carbon-based nanomaterial treatment might be caused by the entry of the trace element Fe and the precipitation of selenoprotein.

4 Discussion

Carbon-based nanoparticles have important research value in integrated systems for tumor diagnosis and treatment because of their unique physical and chemical properties [41, 42]. In recent years, carbon-based nanoparticles have shown certain toxicological effects on the human body and environment [43, 44]. However, there is no clear conclusion regarding the safety of carbon-based drug therapies [45, 46]. Prior studies have shown that high concentrations of SWCNTs and MWCNTs can cause an inflammatory response in the lung tissue, leading to lung tissue injury [47, 48]. Thus, with nanosafety considerations, three different types of carbon-based nanomaterials, namely, GO, SWCNTs, and MWCNTs, were used as research objects. Our group conducted an in vivo animal experiment in SD rats to confirm the enrichment and oxidative damage of the above carbon-based nanoparticles in the rat lung, liver, and brain tissues.

Studies have found that the liver, kidney, lungs, and other organs may be important targets for the enrichment of CNTs, and their metabolites can be excreted through urine [49, 50]. Wang et al. [23] found that SWCNTs were present in vascular endothelial cells and in the bone, stomach, kidney, and other tissues. Warheit [51] and Lam [52] also studied lung injury induced by the respiratory tract injection of unpurified SWCNTs. In this study, the histopathological and TEM results were sufficient to observe the presence of carbon-based nanomaterials in the lungs and liver. The results showed that the substance was enriched in the lungs and could induce an inflammatory response after pulmonary infection. In addition, small amounts of black foreign body materials were found in the rat liver, indicating that carbon-based nanomaterials in different forms can cross the gas–blood barrier and eventually reach the liver tissue (Fig. 10). Carbon-based nanomaterials can be transported with the blood from the lungs to the liver, which plays a key role in the removal of foreign substances. These results are consistent with the previous results [25, 53]. Compared with the liver tissue, there is a tight BBB in the brain tissue, which is an important barrier to prevent various soluble particulates from entering the brain tissue [54, 55]. The SR-μ-XRF results indicated that SWCNTs and MWCNTs may cross the BBB and accumulate in the cortex of the rat brain. This means that SWCNTs and MWCNTs can cross the BBB and enter the systemic circulation, which is consistent with previous results [24, 56]. In a study by Wang et al. [24], MWCNTs broke through most biological barriers, such as the BBB, after caudal vein administration. CNT distribution in the human body differs significantly for various exposure

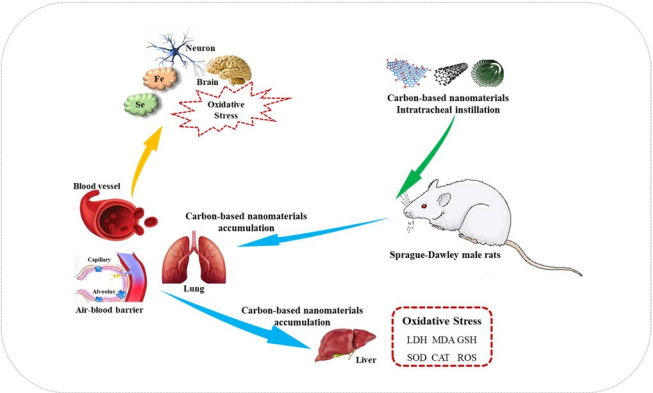

Fig. 10 (Color online) The schematic illustration of the possible pathway of the carbon-based nanomaterials *in vivo*

routes [23]. It has been speculated that their transport in the human body mainly depends on the activity of the blood and macrophages [26]. At the same time, inflammatory cell infiltration, nuclear pyknosis, mitochondrial swelling, and mitochondrial cristae loss were observed in rat liver tissues, and these changes were related to oxidative stress.

Oxidative stress is a key factor in mediating inflammatory cell responses [57]. ROS, as a by-product of energy consumption, played a key role in maintaining homeostasis in the body [58]. These steady states are easily disrupted by external environmental stresses. In our study, ROS levels were increased in the liver and brain. This indicates that the direct instillation of carbon-based nanomaterials into rats could induce ROS generation. In addition, the samples of SWCNTs and MWCNTs in this study contained less than 10 wt.% Fe catalyst and 5 wt.% Fe catalyst, respectively. Studies have shown that transition elements, as the main source of free radicals, have significant toxicological effects on micron particles in ultramicron particles [59]. High levels of ROS can cause serious damage to fat, proteins, DNA, and other tissues in the human body, resulting in heart diseases, neuropathy, and other diseases [15]. The experimental results showed that carbon-based nanomaterials reduced LDH levels and increased MDA levels in the liver and brain. This can damage the biological function of the cell membrane resulting from oxidative damage. GSH is an ubiquitous sulfhydryl-containing molecule in the cells affected by ROS [60]. Some cells may be damaged by the decrease in GSH levels in the liver after carbon-based nanomaterial exposure. In our study, the extra ROS may have induced a large amount of inflammatory cell infiltration in the rat liver tissue and increased mitochondrial volume and mitochondrial vertebral loss. Meanwhile, the ROS could also be quickly eliminated by ROS-scavenging enzymes such as SOD and CAT. SOD converts superoxide anions into hydrogen peroxide and molecular oxygen, and catalase can decomposes these anions into molecular oxygen and water [61, 62]. The activities of SOD and CAT decreased markedly in the presence of carbon-based nanoparticles. Therefore, the extra ROS could be scavenged through antioxidants to maintain the balance of ROS level in the body. In contrast, some researchers [63–65] discussed the safety of the substance and insisted that CNTs were harmless to the human body. In our study, MDA and ROS levels increased slightly in the rat brain after exposure, and the activities of GSH, CAT, and SOD decreased slightly, which was closely related to oxidative stress. Se is well known for its antioxidative capacity; most selenoprotein was in the brain and was mainly distributed in the olfactory bulb, cortex, hippocampus, and cerebellum [32]. Ingold et al. [66] reported that selenocysteine containing GPX4 protects neurons from oxidative stress and ferroptosis. In this study, we found that the deposition of selenoprotein in the rat brain is related to oxidative stress and Fe deficiency.

5 Conclusion

Carbon-based nanomaterials play a critical role in composite nanoelectronic devices, biosensors, biological imaging, and drug delivery. Recently, carbon-based nanomaterials had certain human and ecological risks, and thus, their application in medical treatment is still controversial. In this study, we intended to use different types of carbon-based nanomaterials (GO, SWCNTs, and MWCNTs) as models to observe their distribution and oxidative damage in vivo. Our histopathological and ultrastructural studies indicated that the liver and lungs were the primary accumulation targets of these nanomaterials. The SR-μ-XRF analysis showed that SWCNTs and MWCNTs may also be present in the brain. This shows that the three different types of carbon nanoparticles could pass through the gas–blood barrier and eventually reach the liver tissue. Additionally, SWCNT and MWCNT can cross the BBB and accumulate in the cerebral cortex. The three types of carbon-based nanomaterials may cause oxidative stress in the liver with an increase in ROS and MDA levels along with a decrease in GSH, SOD, and CAT levels. This suggests that direct instillation of these

carbon-based nanomaterials into rats could induce ROS generation. In addition, Fe contaminants in carbon-based nanomaterials are a source of free radicals. However, carbon-based nanoparticles did not cause any discernible damage to the brain tissue of mice, which was similar to the damage to the brain tissue of rats. It has also been shown that the deposition of selenoprotein in the rat brain is related to oxidative stress and Fe deficiency.

Acknowledgements We greatly appreciate the opportunity to measure BL15U of the SSRF in Shanghai, China.

Author Contributions All authors contributed to the study conception and design. Material preparation, data collection and analysis were performed by Ying-Ying Xu, Chan Jin, Meng Wu, Jian-Ye Zhou, and Hui-Ling Wei. The first draft of the manuscript was written by Ying-Ying Xu and all authors commented on previous versions of the manuscript. All authors read and approved the final manuscript.

Data Availibility The data that support the findings of this study are openly available in Science Data Bank at https://cstr.cn/31253.11.sciencedb.j00186.00112 and https://www.doi.org/10.57760/sciencedb.j00186.00112.

Declarations

Conflict of interest The authors declare that they have no Conflict of interest.

References

1. A.M. Dimiev, A. Khannanov, I. Vakhitov et al., Revisiting the mechanism of oxidative unzipping of multiwall carbon nanotubes to graphene nanoribbons. ACS Nano **12**, 3985–3993 (2018). https://doi.org/10.1021/acsnano.8b01617
2. Z. Chen, R. Wu, Y. Liu et al., Ultrafine co nanoparticles encapsulated in carbon-nanotubes-grafted graphene sheets as advanced electrocatalysts for the hydrogen evolution reaction. Adv. Mater. **30**, 1802011 (2018). https://doi.org/10.1002/adma.201802011
3. R. Fang, K. Chen, L. Yin et al., The regulating role of carbon nanotubes and graphene in lithium-ion and lithium-sulfur batteries. Adv. Mater. **31**, 1800863 (2019). https://doi.org/10.1002/adma.201800863
4. Y. Qiao, C.M. Li, S.J. Bao et al., Carbon nanotube/polyaniline composite as anode material for microbial fuel cells. J. Power Sourc. **170**, 79–84 (2007). https://doi.org/10.1016/j.jpowsour.2007.03.048
5. A.K. Ian, S. Jonghwan, L. Jun et al., Composites with carbon nanotubes and graphene: an outlook. Science **362**, 547–553 (2018). https://doi.org/10.1126/science.aat7439
6. V. Sgobba, D.M. Guldi, Carbon nanotubes-electronic/electrochemical properties and application for nanoelectronics and photonics. Chem. Soc. Rev. **38**, 165–184 (2009). https://doi.org/10.1039/b802652c
7. Y. Li, Q. Wei, F. Ma et al., Surface-enhanced Raman nanoparticles for tumor theranostics applications. Acta. Pharm. Sin. B **8**, 349–359 (2018). https://doi.org/10.1016/j.apsb.2018.03.007
8. Y. Yang, J. Zhang, J. Zhuang et al., Synthesis of nitrogen-doped carbon nanostructures from polyurethane sponge for bioimaging and catalysis. Nanoscale **7**, 12284–12290 (2015). https://doi.org/10.1039/c5nr03481g
9. J. Zhao, J. Chen, S. Ma et al., Recent developments in multimodality fluorescence imaging probes. Acta. Pharm. Sin. B **8**, 320–338 (2018). https://doi.org/10.1016/j.apsb.2018.03.010
10. J. Liu, C. Wang, X. Wang et al., Mesoporous silica coated single-walled carbon nanotubes as a multifunctional light-responsive platform for cancer combination therapy. Adv. Funct. Mater. **25**, 384–392 (2015). https://doi.org/10.1002/adfm.201403079
11. B. Newland, C. Taplan, D. Pette et al., Soft and flexible poly(ethylene glycol) nanotubes for local drug delivery. Nanoscale **10**, 8413–8421 (2018). https://doi.org/10.1039/c8nr00603b
12. D. Lombardo, M.A. Kiselev, M.T. Caccamo et al., Smart nanoparticles for drug delivery application: development of versatile nanocarrier platforms in biotechnology and nanomedicine. J. Nanomater. **2019**, 1–26 (2019). https://doi.org/10.1155/2019/3702518
13. M.D. Rakesh, K. Sudhir, N.S. Brahma et al., Carbon nanotubes: a potential concept for drug delivery applications. Recent Pat. Drug Deliv. Formulat. **8**, 12–26 (2014). https://doi.org/10.2174/1872211308666140124095745
14. B. Wan, J. Hou, L. H. Guo, Chapter 14 - Safety of Carbon Nanotubes, Industrial Applications of Carbon Nanotubes, Micro and Nano Technologies, 405–431(2017). https://doi.org/10.1016/B978-0-323-41481-4.00014-9
15. X. He, J. Xue, L. Shi et al., Recent antioxidative nanomaterials toward wound dressing and disease treatment via ROS scavenging. Mater. Today Nano **17**, 100149 (2022). https://doi.org/10.1016/j.mtnano.2021.100149
16. S. Sabra, D.M. Ragab, M.M. Agwa et al., Recent advances in electrospun nanofibers for some biomedical applications. Eur. J. Pharm. Sci. **144**, 105224 (2020). https://doi.org/10.1016/j.ejps.2020.105224
17. A. Galano, Carbon nanotubes as free-radical scavengers. J. Phys. Chem. C **112**, 8922–8927 (2008). https://doi.org/10.1021/jp801379g
18. C. Guo, S. Lv, Y. Liu et al., Biomarkers for the adverse effects on respiratory system health associated with atmospheric particulate matter exposure. J. Hazard. Mater. **421**, 126760 (2022). https://doi.org/10.1016/j.jhazmat.2021.126760
19. A.S. Paul, D.K. Eileen, D.Z. Ralph et al., Focused actions to protect carbon nanotube workers. Am. J. Ind. Med. **55**, 395–411 (2012). https://doi.org/10.1002/ajim.22028
20. M. Saeedi, M. Eslamifar, K. Khezri et al., Applications of nanotechnology in drug delivery to the central nervous system. Biomed. Pharmacother. **111**, 666–675 (2019). https://doi.org/10.1016/j.biopha.2018.12.133
21. P.M. Costa, M. Bourgognon, T.W. Wang et al., Functionalised carbon nanotubes: from intracellular uptake and cell-related toxicity to systemic brain delivery. J. Control Release **241**, 200–219 (2016). https://doi.org/10.1016/j.jconrel.2016.09.033
22. C. Ge, L. Meng, L. Xu et al., Acute pulmonary and moderate cardiovascular responses of spontaneously hypertensive rats after exposure to single-wall carbon nanotubes. Nanotoxicology

6, 526–542 (2012). https://doi.org/10.3109/17435390.2011.587905
23. H. Wang, J. Wang, X. Deng et al., Biodistribution of carbon single-wall carbon nanotubes in mice. J. Nanosci. Nanotechnol. **4**, 1019–1024 (2004). https://doi.org/10.1166/jnn.2004.146
24. H. Kafa, J.T. Wang, N. Rubio et al., The interaction of carbon nanotubes with an in vitro blood-brain barrier model and mouse brain in vivo. Biomaterials **53**, 437–452 (2015). https://doi.org/10.1016/j.biomaterials.2015.02.083
25. X.F. Lu, Y. Zhu, R. Bai et al., Long-term pulmonary exposure to multi-walled carbon nanotubes promotes breast cancer metastatic cascades. Nature Nanotechnol. **14**, 719–727 (2019). https://doi.org/10.1038/s41565-019-0472-4
26. M. Lamberti, P. Pedata, N. Sannolo et al., Carbon nanotubes: properties, biomedical applications, advantages and risks in patients and occupationally-exposed workers. Int. J. Immunopathol. Pharmacol. **28**, 4–13 (2015). https://doi.org/10.1177/0394632015572559
27. M. Boskabady, N. Marefati, T. Farkhondeh et al., The effect of environmental lead exposure on human health and the contribution of inflammatory mechanisms, a review. Environ. Int. **120**, 404–420 (2018). https://doi.org/10.1016/j.envint.2018.08.013
28. Y. Zhu, T.C. Ran, Y.G. Li et al., Observation of growth stimulation of Tetrahymena pyriformis exposed to MWNTs. Nucl. Tech. (in Chinese) **30**, 689–693 (2007)
29. Y. Zhu, Q.F. Zhao, X.Q. Cai et al., Interaction of CNTs with Stylonychia mytilus. Nucl. Tech. (in Chinese) **29**, 202–206 (2006).
30. Y. Zhang, Y. Zhu, Q.N. Li et al., Interaction of metal ions with CNTs and their effects on environmental toxicology. Nucl. Tech. (in Chinese) **34**, 714–720 (2011).
31. O. Shilpa, K.P. Anupama, A. Antony et al., Lead (Pb)-induced oxidative stress mediates sex-specific autistic-like behaviour in Drosophila melanogaster. Mol. Neurobiol. **58**, 6378–6393 (2021). https://doi.org/10.1007/s12035-021-02546-z
32. Y. Zhang, Y. Zhou, U. Schweizer et al., Comparative analysis of selenocysteine machinery and selenoproteome gene expression in mouse brain identifies neurons as key functional sites of selenium in mammals. J. Biol. Chem. **283**, 2427–2438 (2008). https://doi.org/10.1074/jbc.M707951200
33. T. Tian, J.C. Zhang, H.Z. Lei et al., Synchrotron radiation X-ray fluorescence analysis of Fe, Zn and Cu in mice brain associated with Parkinson's disease. Nucl Sci Tech. **26**, 030506 (2015). https://doi.org/10.13538/j.1001-8042/nst.26.030506
34. A.N. Webb, K.M. Spiers, G. Falkenberg et al., Distribution of Pb and Se in mouse brain following subchronic Pb exposure by using synchrotron X-ray fluorescence. Neurotoxicology **88**, 106–115 (2022). https://doi.org/10.1016/j.neuro.2021.11.006
35. I.K. Nina, J.O. Patricia, R.M. Benjamin et al., Layer-by-layer assembly of ultrathin composite films from micron-sized graphite oxide sheets and polycations. Chem. Mater. **11**, 771–778 (1999). https://doi.org/10.1021/cm981085u
36. S. Leila, A. Athawale, Graphene oxide synthesized by using modified hummers approach. Int. J. Energy. Envir. E. **2**, 58–63 (2014)
37. J.F. Colomer, C. Stephan, S. Lefrant et al., Large-scale synthesis of single-wall carbon nanotubes by catalytic chemical vapor deposition CCVD method. Chem. Phys. Lett. **317**, 83–89 (2000). https://doi.org/10.1016/S0009-2614(99)01338-X
38. C. Chen, D. Li, W.C. Lai et al., Standard sample preparation of Pb element determination in atmospheric particles by XRF. Nucl. Tech. (in Chinese) **38**, 120203 (2015). https://doi.org/10.11889/j.0253-3219.2015.hjs.38.120203
39. D. Yang, A. Velamakanni, G. Bozoklu et al., Chemical analysis of graphene oxide films after heat and chemical treatments by X-ray photoelectron and Micro-Raman spectroscopy. Carbon **47**, 145–152 (2009). https://doi.org/10.1016/j.carbon.2008.09.045
40. G. Compagnini, F. Giannazzo, S. Sonde et al., Ion irradiation and defect formation in single layer graphene. Carbon **47**, 3201–3207 (2009). https://doi.org/10.1016/j.carbon.2009.07.033
41. C. Xiang, Y. Zhang, W. Guo et al., Biomimetic carbon nanotubes for neurological disease therapeutics as inherent medication. Acta. Pharm. Sin. B **10**, 239–248 (2020). https://doi.org/10.1016/j.apsb.2019.11.003
42. M.A. Saleemi, Y.L. Kong, P.V.C. Yong et al., An overview of recent development in therapeutic drug carrier system using carbon nanotubes. J. Drug. Deliv. Sci. Technol. **59**, 101855 (2020). https://doi.org/10.1016/j.jddst.2020.101855
43. X. Wang, J.H. Lee, R. Li et al., Toxicological profiling of highly purified single-walled carbon nanotubes with different lengths in the rodent lung and Escherichia Coli. Small **14**, 1703915 (2018). https://doi.org/10.1002/smll.201703915
44. X. Zhang, J. Yin, C. Peng et al., Distribution and biocompatibility studies of graphene oxide in mice after intravenous administration. Carbon **49**, 986–995 (2011). https://doi.org/10.1016/j.carbon.2010.11.005
45. H. Huang, M. Liu, R. Jiang et al., Facile modification of nanodiamonds with hyperbranched polymers based on supramolecular chemistry and their potential for drug delivery. J. Colloid Interface Sci. **513**, 198–204 (2018). https://doi.org/10.1016/j.jcis.2017.11.009
46. R. Jiang, M. Liu, H. Huang et al., Facile fabrication of organic dyed polymer nanoparticles with aggregation-induced emission using an ultrasound-assisted multicomponent reaction and their biological imaging. J. Colloid Interface Sci. **519**, 137–144 (2018). https://doi.org/10.1016/j.jcis.2018.01.084
47. A.A. Shvedova, N. Yanamala, E.R. Kisin et al., Long-term effects of carbon containing engineered nanomaterials and asbestos in the lung: one year postexposure comparisons. Am. J. Physiol. Lung Cell Mol. Physiol. **306**, 170–182 (2014). https://doi.org/10.1152/ajplung.00167.2013
48. R.M. Robert, F.S. James, F.H. Ann et al., Extrapulmonary transport of MWCNT following inhalation exposure. Part. Fibre Toxicol. **10**, 38 (2013). https://doi.org/10.1186/1743-8977-10-38
49. S. Alidori, D.L.J. Thorek, B.J. Beattie et al., Carbon nanotubes exhibit fibrillar pharmacology in primates. PLoS One **12**, 0183902 (2017). https://doi.org/10.1371/journal.pone.0183902
50. Y. Morimoto, M. Horie, N. Kobayashi et al., Inhalation toxicity assessment of carbon-based nanoparticles. Accouc. Chem. Res **46**, 770–781 (2013). https://doi.org/10.1021/ar200311b
51. D.B. Warheit, B.R. Laurence, K.L. Reed et al., Comparative pulmonary toxicity assessment of single-wall carbon nanotubes in rats. Toxicol. Sci. **77**, 117–125 (2004). https://doi.org/10.1093/toxsci/kfg228
52. C.W. Lam, J.T. James, R. Mccluskey et al., Pulmonary toxicity of single-wall carbon nanotubes in mice 7 and 90 days after intratracheal instillation. Toxicol. Sci. **77**, 126–134 (2004). https://doi.org/10.1093/toxsci/kfg243
53. F.D. Wang, L.L. Cao, C. Jin et al., Effects of carbon nanotubes on rat liver and brain. Nano **09**, 1450083 (2014). https://doi.org/10.1142/s1793292014500830
54. B. Obermeier, A. Verma, R.M. Ransohoff, The blood-brain barrier. Handb. Clin. Neurol. **133**, 39–59 (2016). https://doi.org/10.1016/B978-0-444-63432-0.00003-7
55. Z. Guo, P. Zhang, S. Chakraborty et al., Biotransformation modulates the penetration of metallic nanomaterials across an artificial blood-brain barrier model. Proc. Natl. Acad. Sci. USA **118**, 2105245118 (2021). https://doi.org/10.1073/pnas.2105245118
56. S. Deepa, S.K. Mamta, A. Anitha et al., Exposure of carbon nanotubes affects testis and brain of common carp. Environ. Toxicol.

Pharmacol. **95**, 103957 (2022). https://doi.org/10.1016/j.etap.2022.103957
57. M.C. Sanchez, S. Lancel, E. Boulanger et al., Targeting oxidative stress and mitochondrial dysfunction in the treatment of impaired wound healing: a systematic review. Antioxidants **7**, 98 (2018). https://doi.org/10.3390/antiox7080098
58. V.M. Victor, M. Rocha, M. de la Fuente, Immune cells: free radicals and antioxidants in sepsis. Int. Immunopharmacol. **4**, 327–347 (2004). https://doi.org/10.1016/j.intimp.2004.01.020
59. W. Macnee, K. Donaldson, Particulate air Pollution-30: Injurious and protective mechanisms in the lungs. Air Pollut. Health (1999). https://doi.org/10.1016/B978-012352335-8/50105-8
60. O.I. Aruoma, Nutrition and health aspects of free radicals and antioxidants. Fd. Chem. Toxic. **32**, 671–683 (1994). https://doi.org/10.1016/0278-6915(94)90011-6
61. M. Ghorbani, H. Derakhshankhah, S. Jafari et al., Nanozyme antioxidants as emerging alternatives for natural antioxidants: achievements and challenges in perspective. Nano Today **29**, 100775 (2019). https://doi.org/10.1016/j.nantod.2019.100775
62. J. Wu, X. Wang, Q. Wang et al., Nanomaterials with enzyme-like characteristics (nanozymes): next-generation artificial enzymes (II). Chem. Soc. Rev. **48**, 1004–1076 (2019). https://doi.org/10.1039/c8cs00457a
63. S. Prakash, M. Malhotra, W. Shao et al., Polymeric nanohybrids and functionalized carbon nanotubes as drug delivery carriers for cancer therapy. Adv. Drug. Deliv. Rev. **63**, 1340–1351 (2011). https://doi.org/10.1016/j.addr.2011.06.013
64. V. Amenta, K. Aschberger, Carbon nanotubes: potential medical applications and safety concerns. Wiley. Interdiscip. Rev. Nanomed. Nanobiotechnol. **7**, 371–386 (2015). https://doi.org/10.1002/wnan.1317
65. J. Kayat, V. Gajbhiye, R.K. Tekade et al., Pulmonary toxicity of carbon nanotubes: a systematic report. Nanomedicine **7**, 40–49 (2011). https://doi.org/10.1016/j.nano.2010.06.008
66. I. Ingold, C. Berndt, S. Schmitt et al., Selenium utilization by GPX4 Is required to prevent hydroperoxide-induced ferroptosis. Cell **172**, 409–422 (2018). https://doi.org/10.1016/j.cell.2017.11.048